

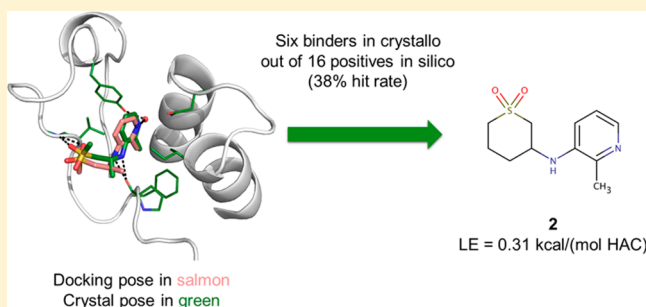
Derivatives of 3-Amino-2-methylpyridine as BAZ2B Bromodomain Ligands: In Silico Discovery and in Crystallo Validation

Jean-Rémy Marchand,[†] Graziano Lolli,^{*,†} and Amedeo Caflisch^{*}

Department of Biochemistry, University of Zürich, Winterthurerstrasse 190, CH-8057, Zürich, Switzerland

Supporting Information

ABSTRACT: The 3-amino-2-methylpyridine derivative **1** was identified as ligand of the BAZ2B bromodomain by automatic docking of nearly 500 compounds, selected on the basis of previous fragment hits. Hit expansion by two in silico approaches, pharmacophore search followed by docking, and substructure search resulted in five additional ligands. The predicted binding mode of the six 3-amino-2-methylpyridine derivatives was validated by protein crystallography. A small displacement of residues 1894–1899 of the ZA loop is observed for two of the six ligands. In all structures, the pyridine head is involved in a water-mediated hydrogen bond with the side chain of the conserved Tyr1901 while the 3-amino linker acts as hydrogen bond donor for the backbone carbonyl of Pro1888. Heterogeneous orientations are observed for the tail groups (i.e., the 3-amino substituents). The sulfonyl group in the tail of compounds **1** and **2** is involved in a hydrogen bond with the backbone amide of Asn1894.



INTRODUCTION

Bromodomains are epigenetic reader modules that bind acetylated lysines (Kac)^{1–4} as well as propionyllysines, butyryllysines, and crotonyllysines⁵ in histones and other proteins. The human genome encodes 61 bromodomains as part of 46 different proteins which contain various additional domains such as histone acetylases, methyltransferases, transcription factors, and helicases.⁶ The members of the BET (bromo and extra terminal domain) subfamily of human bromodomains have been extensively studied in recent years. Potent and selective inhibitors have been developed that proved extremely useful tools for the study of chromatin biology;⁷ due to the involvement of these bromodomains in various malignancies, 12 of these inhibitors are currently tested in clinical trials.⁸ Less is known about the function of other bromodomain-containing proteins such as BAZ2B (bromodomain adjacent to zinc finger domain protein 2B). As for BET bromodomains, the development of potent and selective inhibitors suitable for phenotypic profiling would help uncover the biological role of BAZ2B. These could also prove therapeutically beneficial; single nucleotide polymorphisms in the BAZ2B gene locus have been associated with sudden cardiac death,⁹ while high BAZ2B expression levels were correlated with poor outcome of pediatric B cell acute lymphoblastic leukemia. BAZ2B was reported as one of the least druggable bromodomains due to its unusually small Kac-binding pocket.¹⁰ Two potent BAZ2B inhibitors have been disclosed recently.^{11,12}

In a previous work, we identified by fragment docking four different scaffolds (adenine, imidazole, indole, and indazole) and characterized their binding modes to the BAZ2B pocket by

X-ray crystallography.¹³ With this information in hand, a library of nearly 500 compounds (available for purchase from commercial vendors, see [Methods](#)) was assembled on the basis of the main binding motifs observed in these fragment/BAZ2B complexes (PDB codes 5DYX, 5DYU, 5E9K, 5E9I, and 5E9L). Here we report the identification of a new ligand (the 3-amino-2-methylpyridine derivative **1**, [Table 1](#)) by a combination of flexible ligand docking and validation by X-ray crystallography. In the subsequent hit expansion campaign, five derivatives of **1** were identified as BAZ2B ligands (compounds **2–6**, [Table 1](#)).

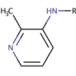
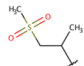
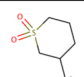
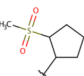
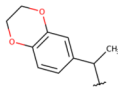
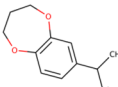
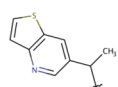
RESULTS AND DISCUSSION

In Silico Screening. A library of 493 molecules was screened in silico by docking ([Figure 1A](#); see [Methods](#) for details). The docked poses were ranked by a force-field-based energy function with approximation of desolvation effects in the continuum-dielectric representation, which led to the selection of seven molecules for further investigation (compound **1** in [Table 1](#) and **10–15** in [Figure S1](#) in the [Supporting Information](#)). These molecules were tested experimentally by soaking in apo crystals of the BAZ2B bromodomain. Electron density for compound **1** was evident in the acetyl-lysine binding pocket ([Figure 2A](#)). Importantly, the binding mode of the 2-methylpyridine headgroup of compound **1** overlaps with the one of 2-chloroimidazole (F275 in our previous fragment-based in silico screening,¹³ PDB code 5E9K, [Figure 2B](#)) which is the fragment that had caused the selection of 45 pyridines for the

Received: August 25, 2016

Published: October 12, 2016

Table 1. In Silico Identified 3-Amino-2-methylpyridine Derivatives Binding to the BAZ2B Bromodomain As Validated by X-ray Crystallography

				
Cmpd (origin)	R group	IC ₅₀ (μM) ^[a]	LE (kcal/mol per heavy atom) ^[b]	PDB code
1 (original hit from primary docking)		> 500	< 0.30	5L96
2 (from substructure search)		279	0.31	5L8T
3 (from substructure search)		> 1000	< 0.24	5L97
4 (from pharmacophore search and secondary docking)		490	0.23	5L98
5 (from pharmacophore search and secondary docking)		ND	ND	5L8U
6 (from pharmacophore search and secondary docking)		481	0.24	5L99

^aSoaking experiments and IC₅₀ (inhibitory concentration for 50% reduction of signal) measurements were performed with racemic mixtures of the compounds. Values of IC₅₀ were measured by the AlphaScreen assay.³⁵ ^bThe ligand efficiency (LE) is the measured binding free energy divided by the number of non-hydrogen atoms.

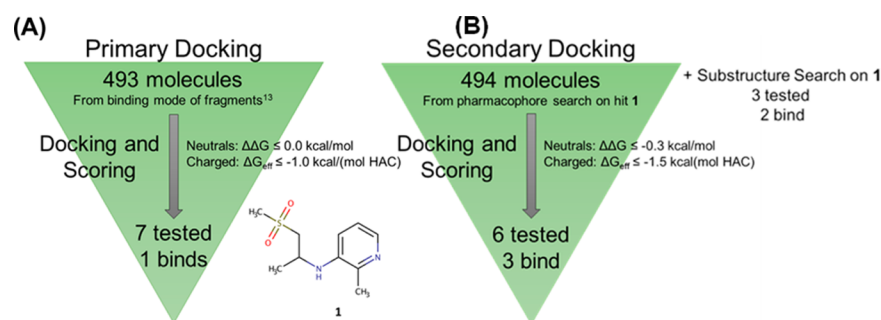


Figure 1. Schematic illustration of the in silico procedures. (A) First a focused library was screened by flexible ligand docking which resulted in the hit **1**. (B) Expansion of hit **1** was performed by two independent approaches in parallel: pharmacophore search followed by docking, and substructure search.

assemblage of the library of 493 compounds. Quantitatively, upon structural alignment of the C α atoms of BAZ2B (PDB codes 5L96 and 5E9K), the distance between the 2-methyl of compound **1** and the chlorine substituent of 2-chloroimidazole is only 0.2 Å. Furthermore, the acceptor atoms that are involved in the water-bridged interaction with Tyr1901 (pyridine nitrogen and imidazole nitrogen in compound **1** and 2-chloroimidazole, respectively) are at a distance of 0.4 Å.

In a second step (hit expansion), a total of 494 compounds was identified in online databases by pharmacophore search using the interactions observed in the crystal structure of the complex between BAZ2B and hit **1** (Figure 1B; see Methods for details). These 494 molecules underwent the same procedure of docking and scoring but with more stringent energy thresholds for final selection. Six compounds survived these filters, and three of them (compounds **4**, **5**, and **6**; Table 1) were confirmed as binders by soaking in apo crystals of

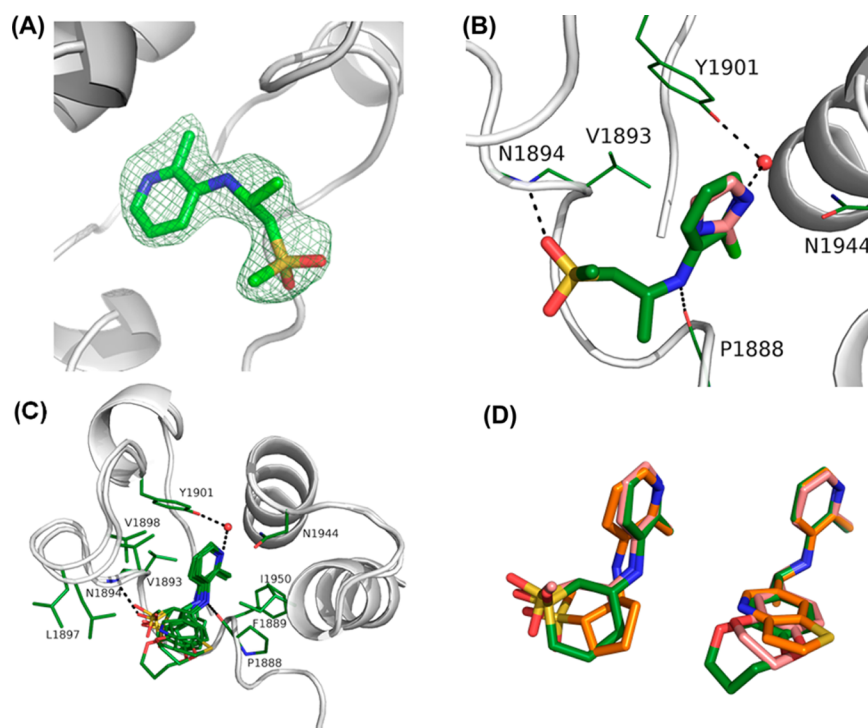


Figure 2. Structural validation of the fragment-based in silico procedure. (A) The *R*-enantiomer of compound 1 in the Kac pocket of the BAZ2B bromodomain is shown with its $F_O - F_C$ map contoured at 3σ . (B) The 2-methylpyridine head of hit 1 (carbon atoms in green) matches the 2-chloroimidazole fragment (carbon atoms in salmon). The structural overlap was obtained by spatial alignment of the C_α atoms of the BAZ2B bromodomain in the complex with 1 (PDB code 5L96) and 2-chloroimidazole (PDB code 5E9K). The backbone NH of Asn1894 and CO of Pro1888 are involved in hydrogen bonds with hit 1. (C) Structural alignment of the six structures of the complexes of the BAZ2B bromodomain with ligands 1–6. The C_α atoms of BAZ2B were used for the alignment. Only two structures of BAZ2B are shown to avoid overcrowding, viz., the structures with ligands 2 and 3. The ZA loop residues 1894–1899 show the largest displacement for ligand 2. The 3-amino-2-methylpyridine derivatives 1–6 show identical binding mode of the headgroup. (D) Zoom-in on ligands 1–3 (left, ligands 1, 2, and 3 with carbon atoms in salmon, green, and orange, respectively) and 4–6 (right, ligands 4, 5, and 6 with carbon atoms in salmon, green, and orange, respectively). All images were rendered using PyMOL, version 1.7.0, Schrödinger LLC.

BAZ2B. Interestingly, despite a diversity of head groups in the library of 494 analogues of hit 1, only one non-pyridine based compound passed the thresholds for selection, the pyrazole derivative 16 (Figure S1 in the Supporting Information) which did not bind to the BAZ2B bromodomain in soaking experiments. In parallel to the hit expansion by secondary docking, a substructure search using hit 1 as query yielded 50 compounds. Three of these 50 derivatives of 3-amino-2-methylpyridine were predicted as binders, and two of them were confirmed by X-ray crystallography (compounds 2 and 3). The 2,6-dimethylpyridine 20 (Figure S1 in the Supporting Information) was selected as negative control because it differs from the hit 1 only by a methyl group (in position 6 of the pyridine ring), which was predicted to bump into the side chain of Phe1943 and Tyr1901. As predicted, compound 20 did not bind to the BAZ2B bromodomain in the soaking experiments.

X-ray Crystallography. In agreement with the docking results, the six crystal structures of the BAZ2B bromodomain/ligand complexes show essentially identical pose and interactions of the 3-amino-2-methylpyridine headgroup (Figure 2C). Its aromatic ring is fully buried within the ZA-loop side chains Val1893 and Tyr1901 on one side of the acetyl-lysine binding site, and Phe1943, Asn1944, and Ile1950 (the so-called gatekeeper) on the other side. The side chain of the gatekeeper has been shown to influence the orientation of the headgroup in a recent study that compared the binding of acetyl indoles in three different bromodomains.¹⁴ The pyridine

nitrogen atom is at a distance of 3.1–3.4 Å from the side chain nitrogen of the conserved asparagine (Asn1944) and is involved in a water-bridged hydrogen bond with the hydroxyl group of the conserved tyrosine (Tyr1901). The 2-methyl substituent is in van der Waals contact with the side chain of Phe1889. The 3-amino group donates a hydrogen bond to the backbone carbonyl of Pro1888. The terminal sulfonyl group of compounds 1 and 2 is involved in a hydrogen bond with the backbone nitrogen of Asn1894; additionally the same group in compound 1 is in hydrogen bond contact with a water molecule bridging it to the main chain carbonyl of Pro1892. The sulfonyl group of compound 3 points in a different orientation with respect to compounds 1 and 2; the hydrogen bond with the backbone nitrogen of Asn1894 is not direct but instead mediated by a bridging water molecule (Figure S2 in the Supporting Information). Another water molecule is tetrahedrally coordinated by the other sulfonyl oxygen of compound 3, the backbone oxygen of Trp1887, and nitrogen atoms of Leu1890 and Leu1891. Compounds 4–6 have double-ring tail groups that are bulkier than the tail groups in 1–3. They are partially solvent exposed and directed toward the exit of the Kac-binding pocket, at an angle of about 90° with respect to the pyridine headgroup. In comparison to compounds 1 and 2, they have reduced interaction with residues toward the end of the ZA loop (Asn1894, Leu1897, and Val1898) while increasing van der Waals and hydrophobic

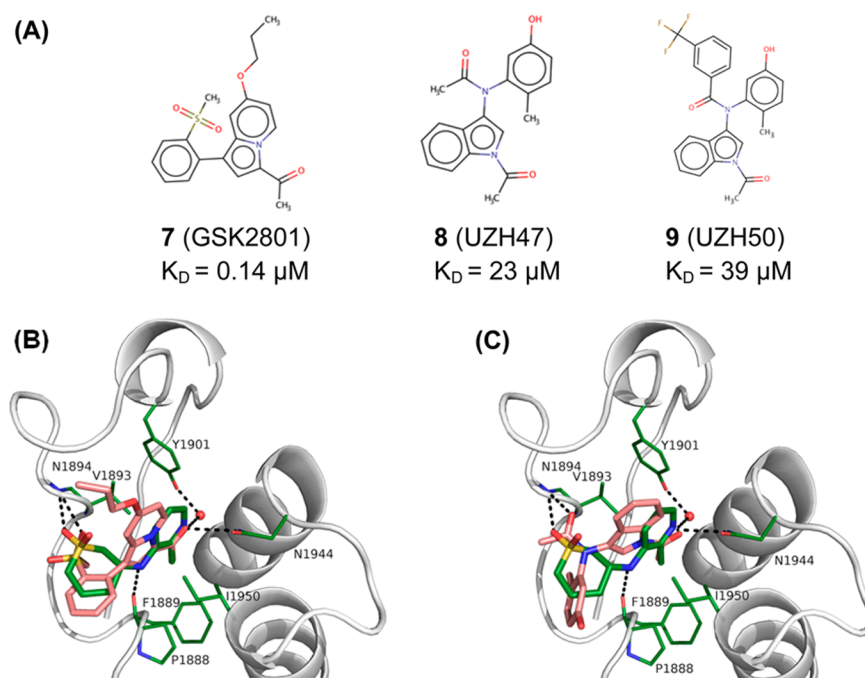


Figure 3. Comparison with selected BAZ2B bromodomain ligands reported in the literature. (A) Chemical structures of the previously disclosed sub- μM inhibitor **7** (affinity measured by ITC)¹² and the low- μM acetyl indole derivatives **8** and **9** (affinity measured by a competition binding assay).¹⁴ (B) Overlap of the structures with the 3-amino-2-methylpyridine derivative **2** (carbon atoms in green, PDB code 5L8T) and the previously disclosed inhibitor **7** (carbon atoms in salmon, PDB code 4RVR). (C) Overlap of **2** (carbon atoms in green, PDB code 5L8T) and the previously disclosed inhibitor **8** (carbon atoms in salmon, PDB code 5E73). The structural alignment is based on the backbone atoms in the α helices.

contacts with residues located on the opposite side of the binding pocket entrance (Trp1887 and Ile1950).

All compounds have a chiral center next to the 3-amino group. In the two highest-resolution structures (compounds **2** and **5** solved to 1.85 Å), electron density strongly indicates that a single enantiomer is present or at least largely predominant. While the *R*-enantiomer is preferred for compound **2**, the *S*-enantiomer of compound **5** is selected. Enantiomeric preference is apparently related to the orientations of the preceding nitrogen toward the carbonyl oxygen of Pro1888 and of the following tail. For the other compounds, the lower resolution (2.15 Å, 2.05 Å, 2.26 Å, and 2.0 Å for the complexes with compounds **1**, **3**, **4**, and **6**, respectively) does not allow us to clearly distinguish between the different enantiomers. However, geometrical and energetic considerations together with the structural analogies with compounds **2** and **5** suggest that the preferred stereoisomer has the *R* configuration for compounds **1** and **3** and the *S* configuration for compounds **4** and **6**. For these four ligands, we cannot exclude that both enantiomers are bound in the crystals in a more balanced ratio.

The structural overlap of the six complexes shows that most of the backbone and chains in the acetyl-lysine binding site are conserved (Figure 2C). In this context, it is important to note that all crystals belong to the same space group and there are no crystal contacts in the acetyl-lysine binding site. The structural similarity in the binding site is very high for the BC-loop (residues 1943–1948) and the first half of the ZA-loop (residues 1887–1893), which starts at the Trp1887-Pro1888-Phe1889 segment (the WPF shelf as in the BET bromodomains). In contrast, the ZA-loop residues 1894–1899 are slightly shifted toward the tail group of the ligand in two of the six structures (compounds **1** and **2**). This displacement is largest for Leu1897 whose C_α atom in the complex with compound **2** is shifted by 1.3 Å from the corresponding atom in

the apo structure (PDB code 3G0L), which was solved in the same space group as our six holo structures. It is interesting to note that the ZA-loop segment 1894–1899 is shifted for the two ligands that make a direct hydrogen bond to the backbone NH of Asn1894 (compounds **1** and **2**, Figure S2 in the Supporting Information) whereas there is no shift for compound **3** which is involved in a water-bridged hydrogen bond with the backbone NH of Asn1894 and compounds **4**–**6** whose tail groups point away from the ZA loop. The side chain of Leu1897 shows two different orientations (tt rotamer, $\chi_1 = -172^\circ$ in the complexes with compounds **1** and **2**; mt rotamer, $\chi_1 = -65^\circ$ in the other structures). Its tip is in contact with the tail group of the ligand in the complexes with compounds **1** and **2** (which is likely to be related also to the aforementioned displacement of the ZA-loop residues 1894–1899), while it points far away from the binding site in the remaining complexes and the apo structure. As observed in 20 crystal structures of the BRPF1 bromodomain in complex with different fragments,¹⁵ the slightly narrower binding pocket in some of the holo structures with respect to the apo conformation is a consequence of the intrinsic plasticity of the ZA-loop and the formation of optimal van der Waals contacts between the ligand and the hydrophobic side chains of Leu1897 and Val1898 on one side of the acetyl-lysine binding pocket and the gatekeeper Ile1950 on the other side (Figure 2C). The side chain of the gatekeeper shows identical position and orientation in all structures, including the apo form (PDB code 3G0L). Thus, minor displacements of part of the ZA-loop are sufficient to accommodate different tail groups of ligands in the BAZ2B bromodomain. It is worth noting that structural disorder of the ZA loop of the BAZ2B bromodomain, as well as other bromodomains, was observed in molecular dynamics simulations by us¹⁶ and others.¹⁷

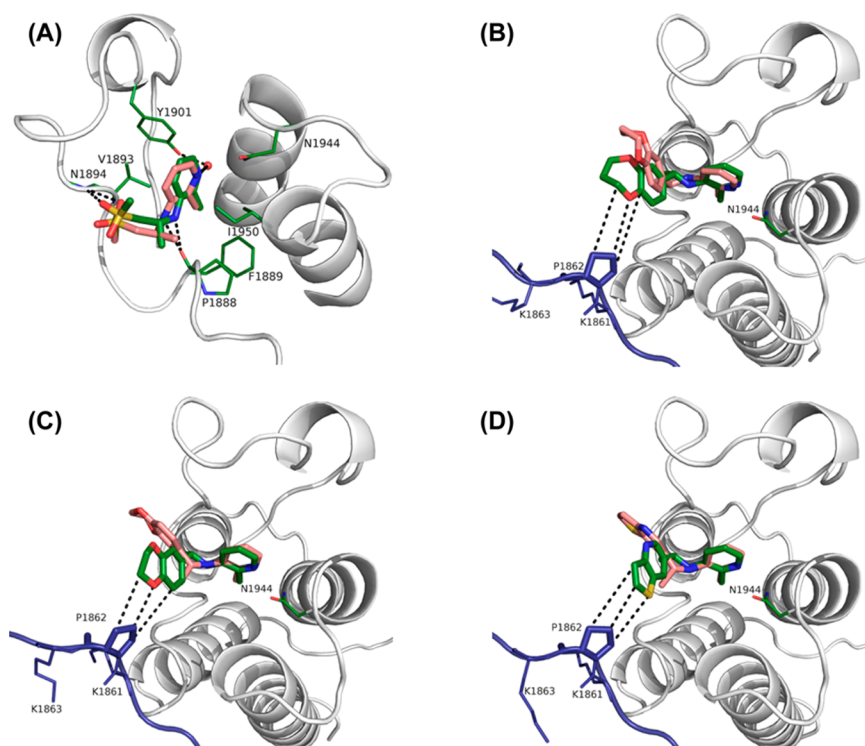


Figure 4. Comparison of docked pose (carbon atoms in salmon) and binding mode observed in the crystal structure (carbon atoms in green). The backbone of the protein chain with the ligand is rendered by a ribbon model (gray), and the neighboring protein chain in the crystal packing is shown with side chains as sticks (dark blue). (A) The docked pose of **1** overlaps with the crystal structure despite the docking was carried out with the enantiomer not observed in the crystal. (B–D) Crystal packing might influence the orientation of the tail groups of **4** (B), **5**(C), and **6** (D).

Comparison with Previously Reported BAZ2B Ligands. It is interesting to compare our inhibitors with the submicromolar compound **7**¹² (Figure 3). The headgroup of our inhibitors contains an aromatic nitrogen atom, which is involved in a water-bridged interaction to the side chain of the conserved Tyr1901, while the oxygen atom of the acetyl group of **7** acts as hydrogen bond acceptor with the structurally conserved water and the side chain of Asn1944. Furthermore, the NH group in position 3 of the pyridine ring, which donates a hydrogen bond to Pro1888, overlaps with an aromatic CH of **7** which is a weaker hydrogen bond donor. Concerning the sulfonyl group of compounds **1–3**, for only inhibitor **3** it points in the same direction as the methylsulfonyl of **7**. On the other hand, as mentioned above, the hydrogen bond to the backbone NH of Asn1894 is water-bridged for compound **3** and direct, as in **7**, for compounds **1** and **2** (Figure 3A) whose sulfonyl groups point in a different orientation than the one of **7**. Instead the orientation of the methylsulfonyl group in compounds **1** and **2** is closer to the central amide linker of recently reported acetylindole ligands **8** and **9** of the BAZ2B bromodomain (Figure 3, PDB codes 5E73 and 5E74, respectively)¹⁴ whose carbonyl group is also involved in a direct hydrogen bond with the backbone nitrogen of Asn1894. Overall, the structural overlaps show that despite their significantly smaller size, our 3-amino-2-methylpyridine-based ligands **1–3** are involved in similar polar interactions with the BAZ2B bromodomain as the previously disclosed **7** and the acetylindole compounds **8** and **9**. In other words, compounds **1–3** efficiently recapitulate the intermolecular hydrogen bonds of significantly larger compounds (ligand efficiency values are discussed below).

It is also interesting to compare our hits to the natural ligand, the Kac of histone tails. Two structures of the BAZ2B bromodomain with acetylated histone peptides have been reported.¹⁸ The hydrogen bonds of the acetyl group of the Kac side chain⁴ are reproduced by our ligands. On the other hand, the interactions with the carbonyl of Pro1888 and the backbone NH of Asn1894 are not observed in the crystal structures with the histone tail (Figure S3 in the Supporting Information).

Comparison of the Docking Poses with the Binding Modes in the Crystal. As mentioned above, the pose of the 3-amino-2-methylpyridine headgroup predicted by docking is essentially identical as in the crystal structures (Figure 4). Contacts between the ligands and the protein are consistent and conserved. Main differences between the docking and crystal poses involve compounds **4–6**, where the tail groups (dihydrobenzodioxine in compound **4**, dihydrobenzodioxepine in **5**, and thienopyridine in **6**) have a different orientation in the crystals. In the crystallographic packing, a symmetric protein chain approaches the exit of the binding pocket with its Pro1862 stacking against Trp1887. A continuous and mostly hydrophobic surface, formed by the two symmetric chains, is presented to the tails of compounds **4–6** (Figure 4B–D). Indeed, Pro1862 from the neighbor chain is as close as 3.7 Å to compound **4**, 3.9 Å to **5**, and 3.8 Å to **6**. These crystallographic contacts could be responsible, at least in part, for the differences in the orientation of the tail groups observed between the docking and the crystallographic poses. Moreover, the degrading electron density for the more external atoms of compounds **4–6**, reflected by their higher *B*-factor values in comparison with the rest of the ligand, indicates high flexibility.

Affinity of the Compounds to the BAZ2B Bromodomain. For racemic mixtures of three of the six compounds,

high micromolar affinity values were measured by the AlphaScreen assay (Table 1 and Figure S4 in the Supporting Information). Compound 2 is the tightest binder with a favorable ligand efficiency¹⁹ of 0.31 kcal/mol per non-hydrogen atom. Its higher affinity with respect to compounds 1 and 3 is consistent with the increased rigidity of the dioxothianyl moiety that favorably orientates its sulfonyl group toward the backbone nitrogen of Asn1894 (in compound 3 the H-bond is not direct but mediated by a water molecule acting as a bridge). This is also reflected by the different mean *B*-factor values of the terminal dimethyl(ene)sulfonyl group in compounds 1–3. In compound 2, this value does not seriously deviate from the rest of the molecule (45 Å² as compared with 34 Å² for the rest of the molecule); in compounds 1 and 3, thermal motions for the five terminal atoms are significantly higher than for the other part of the molecule (71 Å² vs 46 Å² for compound 1 and 83 Å² vs 50 Å² for compound 3). Compounds 4 and 6 show very similar binding affinity. This can be rationalized considering that the most external part of the compounds, where they differ, does not interact with the protein matrix. As such, a very similar binding affinity is expected also for compound 5 (which was not measured).

Because of their different sizes, it is not possible to compare directly the binding affinity of the 3-amino-2-methylpyridine-based ligand 2 (16 non-hydrogen atoms) with the previously disclosed BAZ2B inhibitors 7 (26 non-hydrogen atoms) or the acetylindoles 8 and 9 (24 and 26 non-hydrogen atoms, respectively). By use of the IC₅₀ values obtained by the AlphaScreen assay, the ligand efficiency of compound 2 (0.31 kcal/mol per non-hydrogen atom) is worse than the one of 7 (0.34 kcal/mol per non-hydrogen atom) and more favorable than the one of 8 and 9 (0.26 and 0.27 kcal/mol per non-hydrogen atom, respectively).

CONCLUSIONS

We have used the structural information on fragment binders to the BAZ2B bromodomain to prepare a library of nearly 500 compounds that recapitulate the main interaction motifs observed in our previously reported crystal structures.¹³ Docking of this library followed by hit expansion has resulted in six ligands, which is an overall success rate of 37.5% as only 16 compounds were tested by soaking experiments (Figure 1).

Three main results emerge from the analysis of the crystal structures of the complexes with the original hit 1 and its derivatives 2–6. First, the 3-amino-2-methylpyridine head of compounds 1–6 maintains the orientation and the interactions observed in the original 2-chloroimidazole scaffold¹³ (Figure 2B). The tail groups, which are partially solvent exposed, show heterogeneous orientation.

Second, the hydrogen bond with the backbone NH of Asn1894 can be either direct as for compounds 1 and 2, the two recently disclosed acetylindole ligands 8 and 9 (PDB codes SE73 and SE74, respectively),¹⁴ and the nanomolar ligand 7 (PDB code 4RVR) or water-bridged as in compound 3. Interestingly, the dioxothianyl tail of the strongest binder (i.e., compound 2) is involved in a direct hydrogen bond with the main chain NH of residue 1894 as in 7, although assuming a different orientation (Figure 3B).

Third, the binding site structure is essentially identical in the six structures of compounds 1–6 and the apo form (PDB code 3GOL). A minor rigid-body displacement of residues 1894–1899 of the ZA loop is observed in the structures with compounds 1 and 2 which are the only 3-amino-2-

methylpyridine derivatives that form a direct hydrogen bond with the backbone NH of Asn1894. This displacement is not observed in the structure of the BAZ2B bromodomain in complex with 7 where the ZA loop is superimposable to the apo structure. It is interesting to note that flexibility of the ZA loop was predicted by molecular dynamics simulations.^{16,17}

Taken together, the crystal structures and binding affinity data suggest that optimization of the tail group for the 3-amino-2-methylpyridine head (e.g., by Buchwald–Hartwig amination) will require fine-tuning of the interactions with a subset of backbone polar groups and side chains of the ZA loop. These include hydrogen bonds with the backbone carbonyl of Pro1888 and the backbone amide of Asn1894, and nonpolar interactions with the side chains of Pro1888, Leu1897, and Val1898. Mainly hydrophobic functional groups attached at position 4 and/or position 5 of the 3-amino-2-methylpyridine head could result in favorable nonpolar interactions with the side chains of Leu1897 and Val1898. The (water-bridged) hydrogen bond to the backbone NH of Asn1894 could provide selectivity against human bromodomains that have a Pro at the same position of the ZA loop (e.g., the BRPF1 bromodomain in class IV and members of class V) or a decreased accessibility of that backbone NH group of the ZA loop.

In conclusion, while the high-micromolar affinity is clearly not sufficient for use of these compounds as chemical probes, there is potential for optimization of compound 2 because of its small size (240 g/mol) and good ligand efficiency (0.31 kcal/mol per non-hydrogen atom).

METHODS

Library Assembly and Docking. A library of 493 molecules was assembled manually from commercial vendors on the basis of the main binding motifs observed in a previous fragment-based in silico screening that resulted in crystal structures of complexes with adenine, substituted imidazoles, indoles, and indazoles.¹³ The library consisted of 117 purine, 116 benzopyrazole, 54 imidazole, 45 pyridine, 35 pyrazole, 29 benzimidazole, 26 triazole, 15 imidazolopyridine, 14 benzopyrrole, 10 tetrazole, 8 pyrrolopyridine, 7 pyrrole, 6 piperidine, 5 pyrrolopyrimidine, 2 acylbenzene, 2 benzodiazole, 2 pyrrazolopyridine derivatives. The molecular weight of these molecules ranges from 83 to 503 g/mol with a median of 202 g/mol (Figure S5 in the Supporting Information). The number of rotatable bonds ranges from 0 to 7 with a median of 1. The number of hydrogen bond donors and acceptors ranges from 0 to 5 with a median of 2 and from 1 to 12 with a median of 3, respectively. A total of 1013 tautomers were generated using the calculator plugins of Marvin 15.8.17, 2015, ChemAxon (www.chemaxon.com). The resulting 1013 structures were docked without constraint into the BAZ2B bromodomain Kac binding pocket (PDB code SE73) using RDock,²⁰ 100 runs per molecules. Six water molecules⁴ were kept as part of the bromodomain binding pocket.

The 101 300 docked poses were filtered for a hydrogen bond with the conserved asparagine of the bromodomain (Asn1944) by a Python script. The geometrical thresholds used were <4 Å for the distance between the asparagine side chain nitrogen and any acceptor atom of the docked molecule and >110° for the donor-H-acceptor angle. These rather generous thresholds are appropriate because the docking poses were further minimized. The remaining 19 669 poses (of 482 molecules) were parametrized using the CHARMM general force field CGenFF,²¹ which is fully consistent with CHARMM36 all-atom force field^{22,23} employed for the protein. Docked pose were minimized using CHARMM,²⁴ through 500 steps of steepest descent minimization and 10 000 steps of conjugate gradient minimization, with a tolerance gradient of 0.01 kcal/(mol Å), which was reached in all cases. The dielectric constant was set to 4*r* (where *r* is the distance between atomic nuclei, i.e., positions of partial charges) to take into account the shielding effect of aqueous solvent and still be computationally

efficient.²⁴ Upon minimization, the electrostatic component of the free energy of binding of the docked molecule to the protein was estimated using a single-point calculation of solvation effects with a finite-difference Poisson equation grid-based solver to take into account the presence of solvent within the continuum dielectric approximation.²⁵ The dielectric constant was set to 4 in the protein core and to 78.5 for the water phase. The six explicit water molecules were kept frozen and considered to be part of the solute; i.e., the space occupied by these structural water molecules was assigned a dielectric constant of 4 for the finite-difference Poisson calculation.

Primary in Silico Screening; Identification of the Initial Hit (Compound 1). Charged and neutral compounds were ranked separately because the fixed partial-charge approximation does not capture polarization and induced-charge effects which are more pronounced for compounds with formal charges.²⁶ Compounds without formal charges were discarded if their electrostatic component of the free energy of interaction was less favorable than the free energy of hydration (vacuo to water transfer free energy calculated by the finite-difference Poisson solver), referred later as “ $\Delta\Delta G$ ”. Charged compounds with a calculated binding free energy per non-hydrogen atom (“ ΔG_{eff} ”) less favorable than -1 kcal/(mol HAC), where HAC = heavy atom count, were also filtered out. Only 553 poses (out of 19 669 generated by docking) satisfied these criteria. These 553 poses corresponded to 22 unique molecules, which were visually inspected. Empirically determined as unrealistic binding modes were discarded, compound availability and price were checked, ending with a restricted selection of seven molecules (compound 1 Table 1 and compounds 10–15 Figure S1 in the Supporting Information) to test experimentally.

Selection of Derivatives of the Initial Hit. A total of 494 molecules were selected on the basis of a pharmacophore search. Chemical features of 1 were used on ZINCPharmer:²⁷ position of the hydrogen bond donors and acceptors and the direction from where they can accept/donate hydrogen bonds and the position of hydrophobic core of the pyridine group of 1. The resulting library of 494 analogues of compound 1 was docked and energy minimized as for the primary in silico screening. The only difference was the use of more stringent filters for the minimized poses. The thresholds for neutral compounds was -0.3 kcal/mol (0.0 in the primary in silico screening) and for charged compounds -1.5 kcal/(mol HAC) (-1.0 kcal/(mol HAC) in the primary screening). Six compounds, excluding unavailable molecules, survived these filters and were purchased for further experimental testing (compounds 4–6 Table 1 and compounds 16–18 Figure S1 in the Supporting Information).

In parallel to the selection by pharmacophore search and docking, 50 molecules containing 1 as a substructure were identified on the PubChem database.²⁸ These 50 molecules were not present in the library for the primary in silico screening and were not docked. On the basis of their 2D similarity to 1 and expected interactions, four derivatives of hit 1 were purchased (compounds 2–3 Table 1 and compounds 19 and 20 Figure S1 in the Supporting Information). One of these four molecules, the 2,6-dimethylpyridine 20, differs from 1 by only one additional methyl (in position 6). This additional methyl was predicted not to fit in the BAZ2B bromodomain pocket. Nevertheless, compound 20 was still purchased as negative control because most of the 50 derivatives of 1 have the 2,6-dimethylpyridine head, and compound 20 is the most similar to hit 1.

Compound Purity. All compounds were purchased from ChemSpace. The purity of the molecules was analyzed by HPLC–MS and is $\geq 95\%$.

AlphaScreen Experiments. The AlphaScreen assay consists of a donor bead that is able to transfer singlet oxygen to an acceptor bead that is in the proximity. As a consequence, the acceptor bead emits a luminescent signal. In the presence of a BAZ2B bromodomain ligand, the donor/acceptor complex is disrupted leading to a loss of singlet oxygen transfer and loss of the signal.³⁵ The AlphaScreen assay was carried out at Reaction Biology Inc. using the histone H3 peptide (1-21)K9,K14Ac-biotin-OH. Compounds were tested at 10 doses with 1.5-fold serial dilution starting at 500 μM or 1000 μM .

Protein Production. BAZ2B bromodomain (aa. 1858–1972) was expressed overnight in *E. coli* BL21-DE3 at 18 °C by adding 0.5 mM IPTG to an exponentially growing culture. The 6xHis-tagged protein was purified by coupled DEAE-IMAC and eluted stepwise with increasing concentrations of imidazole. Buffer was exchanged and the tag removed with TEV protease. BAZ2B bromodomain was further purified by a second IMAC and a SEC using a Superdex 75 column. Protein was concentrated to 15 mg/mL and frozen in liquid nitrogen.

Crystallization and Soaking. BAZ2B bromodomain was crystallized by vapor diffusion in sitting drops at 4 °C. Crystallization buffer (pH 7.5) is composed of PEGs of different lengths PEG500MME (18–21%), PEG1000 (0–7%), PEG3350 (0–7%), PEG20000 (9–11%) and also contains MPD (0–7%). Overnight soaking of the compounds was performed by transferring the apo crystals in a soaking solution composed of 32% PEG500MME and 16% PEG20000 in which compounds were previously dissolved. Compounds were tested at 50 mM if soluble at this concentration; less soluble compounds were tested at saturating concentrations. Soaked crystals were frozen in liquid nitrogen. Soaking of the compounds is achieved at the same time with back-soaking of MPD, which is known to bind in the Kac pocket of different bromodomains;¹³ also DMSO was avoided, as it can compete with fragments for the binding in the same site.²⁹

Data Collection and Structure Solution. Diffraction data were collected at the Elettra Synchrotron Light Source (Trieste, Italy), XRD1 beamline. Data were processed with XDS³⁰ and Aimless;³¹ structures were solved by molecular replacement with Phaser³² using PDB code 4IR5 as a search model. Initial models were refined alternating cycles of automatic refinement with Phenix³³ and manual model building with COOT.³⁴ Data collection and refinement statistics are reported in Table S1.

■ ASSOCIATED CONTENT

📄 Supporting Information

The Supporting Information is available free of charge on the ACS Publications Web site: Table S1 and Figures S1–S5. The Supporting Information is available free of charge on the ACS Publications website at DOI: 10.1021/acs.jmedchem.6b01258.

Table S1 listing crystallographic data and refinement statistics and Figures S1–S5 showing structures, binding modes, dose–response curves, and properties of molecules (PDF)

Molecular formula strings and some data (CSV)

Structure data for 1 (PDB)

Structure data for 2 (PDB)

Structure data for 3 (PDB)

Structure data for 4 (PDB)

Structure data for 5 (PDB)

Structure data for 6 (PDB)

Accession Codes

Structures were deposited to the PDB with accession numbers 5L96 (compound 1), 5L8T (compound 2), 5L97 (compound 3), 5L98 (compound 4), 5L8U (compound 5), and 5L99 (compound 6). Authors will release the atomic coordinates and experimental data upon article publication.

■ AUTHOR INFORMATION

Corresponding Authors

*G.L.: e-mail, graziano.lolli@uzh.ch; phone, +41 44 635 55 68.

*A.C.: e-mail, caflisch@bioc.uzh.ch; phone, +41 44 635 55 21.

Author Contributions

†J.-R.M. and G.L. contributed equally to the work.

Notes

The authors declare no competing financial interest.

■ ACKNOWLEDGMENTS

We thank Dr. Dimitrios Spiliotopoulos and Dr. Andrea Unzue for interesting discussions, and Prof. R. Battistutta (University of Padova) for his support. We thank the anonymous reviewers for interesting comments, in particular the correlation between ZA-loop displacement and direct hydrogen bond to the backbone NH of Asn1894. We are grateful to the staff at the XDR1 beamline, ELETTRA Synchrotron Light Source (Trieste, Italy) for on-site assistance. This work was supported in part by a grant from the Swiss Cancer League (Krebsliga Schweiz) and the Swiss National Science Foundation (grant to A.C.).

■ ABBREVIATIONS USED

Kac, acetyl-lysine; BET, bromodomain and extra terminal; BAZ2B, bromodomain adjacent to zinc finger domain protein 2B; LE, ligand efficiency; HAC, heavy atom count

■ REFERENCES

- (1) Haynes, S. R.; Dollard, C.; Winston, F.; Beck, S.; Trowsdale, J.; Dawid, I. B. The bromodomain: a conserved sequence found in human, Drosophila and yeast proteins. *Nucleic Acids Res.* **1992**, *20*, 2603.
- (2) Dhalluin, C.; Carlson, J. E.; Zeng, L.; He, C.; Aggarwal, A. K.; Zhou, M. M. Structure and ligand of a histone acetyltransferase bromodomain. *Nature* **1999**, *399*, 491–496.
- (3) Owen, D. J.; Ornaghi, P.; Yang, J. C.; Lowe, N.; Evans, P. R.; Ballario, P.; Neuhaus, D.; Filetici, P.; Travers, A. A. The structural basis for the recognition of acetylated histone H4 by the bromodomain of histone acetyltransferase gcn5p. *EMBO J.* **2000**, *19*, 6141–6149.
- (4) Marchand, J.-R.; Cafilisch, A. Binding mode of acetylated histones to bromodomains: variations on a common motif. *ChemMedChem* **2015**, *10*, 1327–1333.
- (5) Flynn, E. M.; Huang, O. W.; Poy, F.; Oppikofer, M.; Bellon, S. F.; Tang, Y.; Cochran, A. G. A subset of human bromodomains recognizes butyryllysine and crotonyllysine histone peptide modifications. *Structure* **2015**, *23*, 1801–1814.
- (6) Filippakopoulos, P.; Knapp, S. Targeting bromodomains: epigenetic readers of lysine acetylation. *Nat. Rev. Drug Discovery* **2014**, *13*, 337–356.
- (7) Zhang, G.; Smith, S. G.; Zhou, M.-M. Discovery of chemical inhibitors of human bromodomains. *Chem. Rev.* **2015**, *115*, 11625–11668.
- (8) ClinicalTrials.gov. <http://www.clinicaltrials.gov> (accessed August 25, 2016).
- (9) Arking, D. E.; Juntila, M. J.; Goyette, P.; Huertas-Vazquez, A.; Eijgelsheim, M.; Blom, M. T.; Newton-Cheh, C.; Reinier, K.; Teodorescu, C.; Uy-Evanado, A.; Carter-Monroe, N.; Kaikkonen, K. S.; Kortelainen, M.-L.; Boucher, G.; Lagacé, C.; Moes, A.; Zhao, X.; Kolodgie, F.; Rivadeneira, F.; Hofman, A.; Witteman, J. C. M.; Uitterlinden, A. G.; Marsman, R. F.; Pazoki, R.; Bardai, A.; Koster, R. W.; Dehghan, A.; Hwang, S.-J.; Bhatnagar, P.; Post, W.; Hilton, G.; Prineas, R. J.; Li, M.; Köttgen, A.; Ehret, G.; Boerwinkle, E.; Coresh, J.; Kao, W. H. L.; Psaty, B. M.; Tomaselli, G. F.; Sotoodehnia, N.; Siscovick, D. S.; Burke, G. L.; Marbán, E.; Spooner, P. M.; Cupples, L. A.; Jui, J.; Gunson, K.; Kesäniemi, Y. A.; Wilde, A. A. M.; Tardif, J.-C.; O'Donnell, C. J.; Bezzina, C. R.; Virmani, R.; Stricker, B. H. C. H.; Tan, H. L.; Albert, C. M.; Chakravarti, A.; Rioux, J. D.; Huikuri, H. V.; Chugh, S. S. Identification of a sudden cardiac death susceptibility locus at 2q24.2 through genome-wide association in European ancestry individuals. *PLoS Genet.* **2011**, *7*, e1002158.
- (10) Ferguson, F. M.; Fedorov, O.; Chaikuad, A.; Philpott, M.; Muniz, J. R. C.; Felletar, I.; von Delft, F.; Heightman, T.; Knapp, S.; Abell, C.; Ciulli, A. Targeting low-druggability bromodomains: fragment based screening and inhibitor design against the BAZ2B bromodomain. *J. Med. Chem.* **2013**, *56*, 10183–10187.
- (11) Drouin, L.; McGrath, S.; Vidler, L. R.; Chaikuad, A.; Monteiro, O.; Tallant, C.; Philpott, M.; Rogers, C.; Fedorov, O.; Liu, M.; Akhtar, W.; Hayes, A.; Raynaud, F.; Müller, S.; Knapp, S.; Hoelder, S. Structure enabled design of BAZ2-ICR, a chemical probe targeting the bromodomains of BAZ2A and BAZ2B. *J. Med. Chem.* **2015**, *58*, 2553–2559.
- (12) Chen, P.; Chaikuad, A.; Bamborough, P.; Bantscheff, M.; Bountra, C.; Chung, C.-W.; Fedorov, O.; Grandi, P.; Jung, D.; Lesniak, R.; Lindon, M.; Müller, S.; Philpott, M.; Prinjha, R.; Rogers, C.; Selenski, C.; Tallant, C.; Werner, T.; Willson, T. M.; Knapp, S.; Drewry, D. H. Discovery and characterization of GSK2801, a selective chemical probe for the bromodomains BAZ2A and BAZ2B. *J. Med. Chem.* **2016**, *59*, 1410–1424.
- (13) Lolli, G.; Cafilisch, A. High-throughput fragment docking into the BAZ2B bromodomain: efficient in silico screening for X-ray crystallography. *ACS Chem. Biol.* **2016**, *11*, 800–807.
- (14) Unzue, A.; Zhao, H.; Lolli, G.; Dong, J.; Zhu, J.; Zechner, M.; Dolbois, A.; Cafilisch, A.; Nevado, C. The “gatekeeper” residue influences the binding mode of acetyl indoles to bromodomains. *J. Med. Chem.* **2016**, *59*, 3087–3097.
- (15) Zhu, J.; Cafilisch, A. Twenty crystal structures of bromodomain and PHD finger containing protein 1 (BRPF1)/ligand complexes reveal conserved binding motifs and rare interactions. *J. Med. Chem.* **2016**, *59*, 5555–5561.
- (16) Steiner, S.; Magno, A.; Huang, D.; Cafilisch, A. Does bromodomain flexibility influence histone recognition? *FEBS Lett.* **2013**, *587*, 2158–2163.
- (17) Ferguson, F. M.; Dias, D. M.; Rodrigues, J. P.; Wienk, H.; Boelens, R.; Bonvin, A. M.; Abell, C.; Ciulli, A. Binding hotspots of BAZ2B bromodomain: histone interaction revealed by solution NMR driven docking. *Biochemistry* **2014**, *53*, 6706–6716.
- (18) Tallant, C.; Valentini, E.; Fedorov, O.; Overvoorde, L.; Ferguson, F. M.; Filippakopoulos, P.; Svergun, D. I.; Knapp, S.; Ciulli, A. Molecular basis of histone tail recognition by human TIP5 PHD finger and bromodomain of the chromatin remodeling complex NoRC. *Structure* **2015**, *23*, 80–92.
- (19) Hopkins, A. L.; Groom, C. R.; Alex, A. Ligand efficiency: a useful metric for lead selection. *Drug Discovery Today* **2004**, *9*, 430–431.
- (20) Ruiz-Carmona, S.; Alvarez-Garcia, D.; Foleppé, N.; Garmendia-Doval, A. B.; Juho, S.; Schmidtke, P.; Barril, X.; Hubbard, R. E.; Morley, S. D. rDock: a fast, versatile and open source program for docking ligands to proteins and nucleic acids. *PLoS Comput. Biol.* **2014**, *10*, e1003571.
- (21) Vanommeslaeghe, K.; Hatcher, E.; Acharya, C.; Kundu, S.; Zhong, S.; Shim, J.; Darian, E.; Guvench, O.; Lopes, P.; Vorobyov, I.; Mackerell, A. D., Jr. CHARMM general force field: a force field for drug-like molecules compatible with the CHARMM all-atom additive biological force fields. *J. Comput. Chem.* **2010**, *31*, 671–690.
- (22) MacKerell, A. D.; Bashford, D.; Bellott, M.; Dunbrack, R. L.; Evanseck, J. D.; Field, M. J.; Fischer, S.; Gao, J.; Guo, H.; Ha, S.; Joseph-McCarthy, D.; Kuchnir, L.; Kuczera, K.; Lau, F. T.; Mattos, C.; Michnick, S.; Ngo, T.; Nguyen, D. T.; Prodhom, B.; Reiher, W. E.; Roux, B.; Schlenkrich, M.; Smith, J. C.; Stote, R.; Straub, J.; Watanabe, M.; Wiórkiewicz-Kuczera, J.; Yin, D.; Karplus, M. All-atom empirical potential for molecular modeling and dynamics studies of proteins. *J. Phys. Chem. B* **1998**, *102*, 3586–3616.
- (23) MacKerell, A. D., Jr.; Feig, M.; Brooks, C. L., III. Improved treatment of the protein backbone in empirical force fields. *J. Am. Chem. Soc.* **2004**, *126*, 698–699.
- (24) Brooks, B. R.; Brooks, C. L., III; Mackerell, A. D., Jr.; Nilsson, L.; Petrella, R. J.; Roux, B.; Won, Y.; Archontis, G.; Bartels, C.; Boresch, S.; Cafilisch, A.; Caves, L.; Cui, Q.; Dinner, A. R.; Feig, M.; Fischer, S.; Gao, J.; Hodoscek, M.; Im, W.; Kuczera, K.; Lazaridis, T.; Ma, J.; Ovchinnikov, V.; Paci, E.; Pastor, R. W.; Post, C. B.; Pu, J. Z.; Schaefer, M.; Tidor, B.; Venable, R. M.; Woodcock, H. L.; Wu, X.; Yang, W.; York, D. M.; Karplus, M. CHARMM: the biomolecular simulation program. *J. Comput. Chem.* **2009**, *30*, 1545–1614.

- (25) Im, W.; Beglov, D.; Roux, B. Continuum solvation model: computation of electrostatic forces from numerical solutions to the Poisson-Boltzmann equation. *Comput. Phys. Commun.* **1998**, *111*, 59–75.
- (26) Zhou, T.; Huang, D.; Caflisch, A. Is quantum mechanics necessary for predicting binding free energy? *J. Med. Chem.* **2008**, *51*, 4280–4288.
- (27) Koes, D. R.; Camacho, C. J. ZINCPharmer: pharmacophore search of the ZINC database. *Nucleic Acids Res.* **2012**, *40*, W409–W414.
- (28) Kim, S.; Thiessen, P. A.; Bolton, E. E.; Chen, J.; Fu, G.; Gindulyte, A.; Han, L.; He, J.; He, S.; Shoemaker, B. A.; Wang, J.; Yu, B.; Zhang, J.; Bryant, S. H. PubChem substance and compound databases. *Nucleic Acids Res.* **2016**, *44*, D1202–D1213.
- (29) Lolli, G.; Battistutta, R. Different orientations of low-molecular-weight fragments in the binding pocket of a BRD4 bromodomain. *Acta Crystallogr., Sect. D: Biol. Crystallogr.* **2013**, *69*, 2161–2164.
- (30) Kabsch, W. XDS. *Acta Crystallogr., Sect. D: Biol. Crystallogr.* **2010**, *66*, 125–132.
- (31) Evans, P. R.; Murshudov, G. N. How good are my data and what is the resolution? *Acta Crystallogr., Sect. D: Biol. Crystallogr.* **2013**, *69*, 1204–1214.
- (32) McCoy, A. J.; Grosse-Kunstleve, R. W.; Adams, P. D.; Winn, M. D.; Storoni, L. C.; Read, R. J. Phaser crystallographic software. *J. Appl. Crystallogr.* **2007**, *40*, 658–674.
- (33) Adams, P. D.; Afonine, P. V.; Bunkóczi, G.; Chen, V. B.; Davis, I. W.; Echols, N.; Headd, J. J.; Hung, L.-W.; Kapral, G. J.; Grosse-Kunstleve, R. W.; McCoy, A. J.; Moriarty, N. W.; Oeffner, R.; Read, R. J.; Richardson, D. C.; Richardson, J. S.; Terwilliger, T. C.; Zwart, P. H. PHENIX: a comprehensive Python-based system for macromolecular structure solution. *Acta Crystallogr., Sect. D: Biol. Crystallogr.* **2010**, *66*, 213–221.
- (34) Emsley, P.; Lohkamp, B.; Scott, W. G.; Cowtan, K. Features and development of Coot. *Acta Crystallogr., Sect. D: Biol. Crystallogr.* **2010**, *66*, 486–501.
- (35) Philpott, M.; Yang, J.; Tumber, T.; Fedorov, O.; Uttarkar, S.; Filippakopoulos, P.; Picaud, S.; Keates, T.; Felletar, I.; Ciulli, A.; Knapp, S.; Heightman, T. D. Bromodomain-peptide displacement assays for interactome mapping and inhibitor discovery. *Mol. BioSyst.* **2011**, *7*, 2899–2908.